

The Maximum Entropy Relaxation Path

Moshe Dubiner

MOSHE@GOOGLE.COM

Google Inc.

1600 Amphitheater Parkway

Mountain View, CA 94043, USA

Matan Gavish

GAVISH@STANFORD.EDU

Department of Statistics

Stanford University

Stanford, CA 94305, USA

Yoram Singer

SINGER@GOOGLE.COM

Google Inc.

1600 Amphitheater Parkway

Mountain View, CA 94043, USA

Abstract

The relaxed maximum entropy problem is concerned with finding a probability distribution on a finite set that minimizes the relative entropy to a given prior distribution, while satisfying relaxed max-norm constraints with respect to a third observed multinomial distribution. We study the entire relaxation path for this problem in detail. We show existence and a geometric description of the relaxation path. Specifically, we show that the maximum entropy relaxation path admits a planar geometric description as an increasing, piecewise linear function in the inverse relaxation parameter. We derive fast algorithms for tracking the path. In various realistic settings, our algorithms require $O(n \log(n))$ operations for probability distributions on n points, making it possible to handle large problems. Once the path has been recovered, we show that given a validation set, the family of admissible models is reduced from an infinite family to a small, discrete set. We demonstrate the merits of our approach in experiments with synthetic data and discuss its potential for the estimation of compact n-gram language models.

1. Introduction

This paper studies the set of solutions to the relaxed maximum entropy problem

$$\begin{aligned} \min_{\mathbf{p} \in \Delta} \quad & \sum_{j=1}^n p_j \log \left(\frac{p_j}{u_j} \right) \\ \text{s.t.} \quad & \|\mathbf{p} - \mathbf{q}\|_{\infty} \leq 1/\nu, \end{aligned} \tag{1}$$

where Δ is the probability simplex in \mathbb{R}^n , and where $\mathbf{q}, \mathbf{u} \in \Delta$ are given. The solution set, indexed by the relaxation parameter $\nu \geq 0$, is known as the *relaxation path* of (1).

Numerous machine learning tasks are cast as an optimization problem, similar to the form above, in which the objective decomposes into an empirical risk function, and an added regularization term, which controls the model complexity. The tradeoff between risk and model complexity is determined by a scalar relaxation parameter, which is often tuned by solving the optimization problem for multiple relaxation parameter values, and using a validation set in order to choose the most appropriate one. An alternative approach is to characterize the solution for *any* possible relaxation parameter, effectively solving the problem for all values simultaneously. This characterization is known in the literature as a solution for the entire regularization (or relaxation) path.

Characterization of the entire relaxation path of specific problems has been the focus of a relatively small number of research papers. Concretely, Osborne et al. (2000a) and Efron et al. (2004) provide two different characterizations of the entire relaxation path of the Lasso (Tibshirani, 1996). Osborne et al. (2000b) called the mapping between the space of regularization values to the set of solutions *Homotopy*, a term that we adopt here. In the context of support vector machines, Pontil and Verri (1998) and Hastie et al. (2004) characterized the relaxation path observed for SVM. Rosset and Zhu (2007) gave a general characterization for losses which admit a linear relaxation path. Rosset (2004) described an approximate characterization for the relaxation path of logistic regression and related problems. Zhao and Yu (2004) provided an approximate characterization of the relaxation path for any convex loss function with an additive ℓ_1 regularization term. Park and Hastie (2007) provided an approximate characterization of the relaxation path for generalized linear models. More recently, Tibshirani and Taylor (2011) characterized the relaxation path for a generalized Lasso problem where the ℓ_1 penalty is applied to a linear transformation of the Lasso variables.

In this paper we study a specific problem, in which the objective term is additively separable. Throughout most of the paper we focus on the case where the objective is the relative entropy between two multinomial distributions with a max-norm constraint, known as the *relaxed maximum entropy* problem. The general form of maximum entropy subject to relaxed constraints was studied in (Dudík et al., 2007). Dudík et al. described a general account for relaxed maximum entropy prob-

lems and derived corresponding generalization bounds. For other related relaxation approaches see also Sec. 1.1 in (Dudík et al., 2007).

The paper proceeds as follows. In Sec. 2 we study the general case of additively separable convex objective. We show that in this generality, the relaxation path exists and is given as the solution to an equation in the inverse relaxation parameter. In Sec. 3 we show that the maximum entropy relaxation path admits a simple planar geometric characterization in the inverse relaxation parameter, as an increasing, piecewise linear function. In Sec. 4 we build on the geometrical description and derive a path tracking algorithm with worst-case time complexity $O(n^3)$ for vectors of length n . Specializations of the general algorithms are provided, which are able in realistic cases to recover the path in time complexity $O(n \log(n))$, making it possible to handle very large maximum entropy problems. In Sec. 5 we describe an efficient cross-validation procedure based on the entire path solution: by solving for the relaxation path, given a validation set, we are able to reduce the family of admissible models, which are considered for model selection, from an infinite family to a small, discrete set. In Sec. 6 we illustrate the merits of our approach in experiments with synthetic data. Sec. 7 describes an application of our approach for estimation of compact n-gram language models. In Sec. 8 we describe extensions, including a different case in which the relaxation path exists and can be tracked efficiently. Finally, in Appendix A we provide a more complicated path tracking algorithm, with improved worst-case computational time complexity $O(n^2 \log(n))$.

2. The Relaxation Path: Basic Properties

2.1 Notation

We denote vectors with bold face letter, e.g. \mathbf{v} . Sums are denoted by calligraphic letters, e.g. $\mathcal{M} = \sum_j m_j$. We use the shorthand $[n]$ to denote the set of integers $\{1, \dots, n\}$. The inner-product between two vectors \mathbf{u} and \mathbf{v} is denoted, $\mathbf{u} \cdot \mathbf{v}$. The *generalized* simplex with respect to a vector \mathbf{m} whose components are positive is $\Delta(\mathbf{m}) = \{\mathbf{p} \mid \mathbf{p} \cdot \mathbf{m} = 1, \forall j : p_j \geq 0\}$. Note that when for all j , $m_j = 1$, we get the standard definition of the simplex. Similarly, when for all j , $m_j = \frac{1}{R}$, we retrieve the positive part of the ℓ_1 ball of radius R . We call \mathbf{m} the multiplicity vector. As the name implies, its role is to incorporate the case where there are repeated entries in \mathbf{p} which take the same values. These repeated values are encoded by setting their multiplicity accordingly. An addition rationale for allowing multiplicity vectors is given in Sec. 8.

2.2 General Solution Characterization

Consider first the following generalized form of problem 1:

$$\min_{\mathbf{p} \in \Delta(\mathbf{m})} \phi(\mathbf{p}) \quad \text{s.t.} \quad \|\mathbf{p} - \mathbf{q}\|_\infty \leq 1/\nu, \quad (2)$$

where $\mathbf{q}, \mathbf{u} \in \Delta(\mathbf{m})$ are given probability vectors, and ϕ is a strictly convex function. This form is a convenient apparatus for describing the general properties of the solution.

Clearly, since for any $\nu \geq 0$ the objective function of (2) is a strictly convex function over a compact convex domain, its optimum $\mathbf{p}(\nu)$ exists. Further, it is unique and can be viewed as a continuous vector function in ν . Let us now further characterize the form of the solution \mathbf{p} . We can partition the set of indices in $[n]$ into three disjoint sets depending on whether either of the max-norm constraints $p_j - q_j \leq 1/\nu$ or $p_j - q_j \geq -1/\nu$ is binding:

$$\begin{aligned} I_-(\nu) &= \{1 \leq j \leq n \mid p_j = q_j - 1/\nu\} \\ I_0(\nu) &= \{1 \leq j \leq n \mid |p_j - q_j| < 1/\nu\} \\ I_+(\nu) &= \{1 \leq j \leq n \mid p_j = q_j + 1/\nu\} . \end{aligned} \tag{3}$$

An alternative form of representing the partition (I_-, I_0, I_+) is obtained by associating an indicator value with each coordinate resulting in a vector $\mathbf{s} \in \{-1, 0, 1\}^n$ where

$$s_j = \begin{cases} -1 & j \in I_- \\ 0 & j \in I_0 \\ +1 & j \in I_+ \end{cases} .$$

We make use of both notations. Our goal is to devise an algorithmic infrastructure that lets us reveal the correct partition without examining all of the 3^n possible partitions. The following characterizes the gradient of solution in terms of the partition (I_-, I_0, I_+) .

Lemma 1 *Let $\mathbf{p} \in \Delta(\mathbf{m})$, ϕ be a strictly convex function, and $\nu > 0$. Assume that ϕ is differentiable over $\Delta(\mathbf{m})$, and that its optimum has no zero coordinates. Let $\partial_j \phi = \frac{\partial \phi}{\partial p_j}$ denote the j -th coordinate of the gradient of ϕ . Then, \mathbf{p} minimizes (2) iff there exists $-\infty < \eta < \infty$ such that for any $1 \leq j \leq n$ exactly one of the following three conditions holds,*

$$\partial_j \phi(\mathbf{p}) \geq \eta m_j \quad \text{if} \quad p_j = q_j - 1/\nu \tag{4}$$

$$\partial_j \phi(\mathbf{p}) = \eta m_j \quad \text{if} \quad |p_j - q_j| < 1/\nu \tag{5}$$

$$\partial_j \phi(\mathbf{p}) \leq \eta m_j \quad \text{if} \quad p_j = q_j + 1/\nu . \tag{6}$$

Proof We prove the lemma by using of the complementary slackness conditions for optimality. For brevity we assume throughout the rest of the proof that $m_j = 1$ for all $j \in [n]$. We associate a Lagrange multiplier $\alpha_j^+ \geq 0$ for the constraint $p_j - q_j \leq 1/\nu$ and $\alpha_j^- \geq 0$ for the constraint $p_j - q_j \geq -1/\nu$. We use η to denote the Lagrange multiplier for the simplex constraint $\sum_j p_j = 1$. Since we assumed that the solution is strictly positive, we know that the Lagrange multipliers corresponding

to the positivity constraints of \mathbf{p} would be all zero at min-max saddle point of the Lagrangian. Hence, we get the following Lagrangian,

$$\mathcal{L} = \phi(\mathbf{p}) + \sum_{j=1}^m \alpha_j^+(p_j - q_j - 1/\nu) - \sum_{j=1}^m \alpha_j^-(p_j - q_j + 1/\nu) - \eta \left(\sum_{j=1}^n p_j - 1 \right) .$$

From the necessary condition for optimality we know that $\partial \mathcal{L} / \partial p_j = 0$ for all $j \in [n]$. Therefore, we get that for all indices j the following holds at the optimum,

$$\partial_j \phi(\mathbf{p}) + \alpha_j^+ - \alpha_j^- + \eta = 0 . \quad (7)$$

We now need to examine three cases, depending on the relation between p_j and q_j . First, when $|p_j - q_j| < 1/\nu$, neither of the inequality constraints is binding. Therefore, the complementary slackness conditions imply that at the saddle point $\alpha_j^+(p_j - q_j - 1/\nu) = 0$ and $\alpha_j^-(p_j - q_j + 1/\nu) = 0$. We thus must have $\alpha_j^+ = \alpha_j^- = 0$ at the optimum. In this case, $\partial_j \phi(\mathbf{p}) = \eta$ which is case (5) in the theorem statement. Next, if $p_j - q_j = 1/\eta$, then $\alpha_j^- = 0$ while $\alpha_j^+ \geq 0$, using again the complementary slackness conditions for optimality. We therefore get that $\partial_j \phi(\mathbf{p}) = \eta - \alpha_j^+ \leq \eta$ which is case (6) of the problem statement. The case $p_j - q_j = -1/\nu$ is derived analogously. Finally, when $\mathbf{m} \neq \mathbf{1}$ we modify the simplex constraint accordingly and replace α_j^\pm with $m_j \alpha_j^\pm$. \blacksquare

The above lemma provides us with a simple certificate for the optimality of a vector \mathbf{p} , given I_- , I_0 , I_+ and ν . As we will see the partition tends to remain intact as ν varies. This makes it possible to track the solution path $\mathbf{p}(\nu)$ as ν gradually increases. This approach is known as the Homotopy method (Osborne et al., 2000b).

2.3 Relaxation Path for Additively Separable Convex Objectives

We now arrive at the notion of a relaxation path. It is convenient to keep the discussion general before narrowing down to our main subject, the relaxed maximal entropy problem. We restrict the objective $\phi(\cdot)$ from (2) to the case of an additively separable function,

$$\phi(\mathbf{p}) = \sum_{j=1}^n m_j \phi_j(p_j) . \quad (8)$$

We further constrain each function $\phi_j : \mathbb{R} \rightarrow \mathbb{R}$ and assume that it is a strictly convex and continuously differentiable over $(0, 1)$.

Existence of the relaxation path. Under these conditions, we now show that there exists a function $\nu \mapsto \eta(\nu)$ defined over an interval $[0, \nu_\infty]$, given implicitly as the unique solution to equation (11) below, which completely determines the solution $\mathbf{p}(\nu)$ to (2), through the relation

$$p_j(\nu) = q_j + \frac{1}{\nu} \theta(\nu \psi_j(\eta(\nu)) - \nu q_j)$$

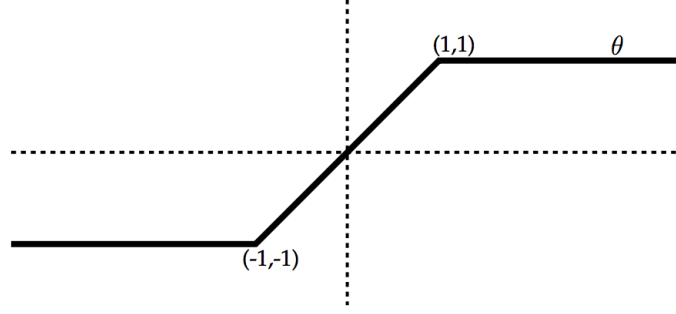


Figure 1: The capping function θ .

where the functions $\theta(\cdot)$ and $\psi_j(\cdot)$ are given explicitly in the sequel. Thus, the term “path” for $\nu \mapsto \eta(\nu)$ is justified, since knowledge of $\eta(\nu)$ allows us to determine $\mathbf{p}(\nu)$ instantly. We now unravel the structure of $\theta(\cdot)$ and $\psi_j(\cdot)$.

Given the assumption on the functions ϕ_j , $\frac{d\phi_j(p_j)}{dp_j}$ is a monotonically increasing continuous function. Let $0 \leq \psi_j \leq 1$ denote its inverse function, i.e.,

$$\psi_j \left(\frac{d\phi_j(p_j)}{dp_j} \right) = p_j \quad \text{for } 0 < p_j < 1 \quad .$$

We can now invoke Lemma 1 and characterize the correct partition (I_-, I_0, I_+) in terms of the inverse function ψ as follows:

$$\begin{aligned} p_j &\geq \psi_j(\eta) & j &\in I_- \\ p_j &= \psi_j(\eta) & j &\in I_0 \\ p_j &\leq \psi_j(\eta) & j &\in I_+ \end{aligned}$$

which implies that

$$p_j = \begin{cases} q_j - 1/\nu & \psi_j(\eta) \leq q_j - 1/\nu \\ \psi_j(\eta) & |\psi_j(\eta) - q_j| < 1/\nu \\ q_j + 1/\nu & \psi_j(\eta) \geq q_j + 1/\nu \end{cases} \quad . \quad (9)$$

Denote by $\theta(\cdot)$ the capping function

$$\theta(x) = \max \{-1, \min \{1, x\}\} \quad .$$

An illustration of the capping function is given in Fig. 1. Equipped with this definition we can rewrite (9) as follows

$$\forall j \in [n] : \quad p_j = q_j + \frac{1}{\nu} \theta(\nu \psi_j(\eta) - \nu q_j) \quad . \quad (10)$$

The solution is thus completely determined by a single unknown parameter η , which depends on the problem variables and on ν . We now use the fact that that \mathbf{q} and \mathbf{p} are in $\Delta(\mathbf{m})$, sum (10) over j , and get

$$\underbrace{\sum_{j=1}^n m_j p_j}_{=1} = \underbrace{\sum_{j=1}^n m_j q_j}_{=1} + \frac{1}{\nu} \sum_{j=1}^n m_j \theta(\nu \psi_j(\eta) - \nu q_j) .$$

The above equality leads to the following implicit equation for determining η

$$G(\nu, \eta) \stackrel{\text{def}}{=} \sum_{j=1}^n m_j \theta(\nu \psi_j(\eta) - \nu q_j) = 0 . \quad (11)$$

The correct value for η is obtained by finding a zero of $G(\nu, \cdot)$. The solution of $G(\nu, \eta) = 0$ would give rise to the unique optimal \mathbf{p} through (10). Since the continuous function $G(\nu, \eta)$ is monotonically non-decreasing from $G(\nu, -\infty) \leq 0$ to $G(\nu, \infty) \geq 0$, a solution (w.r.t. η) to the equation $G(\nu, \eta) = 0$ exists. Moreover, the functions $\psi_j(\eta)$ are monotonically increasing, thus the only setting in which we may obtain multiple solutions occurs when the capping function is in its “flat” region. This can happen only if the set I_0 is empty, thus $p_j = q_j \pm 1/\nu$. Let

$$\nu_\infty \stackrel{\text{def}}{=} \inf \{ \nu \geq 0 \mid I_0(\nu) = \emptyset \} . \quad (12)$$

If the set I_0 is never empty for all finite values of ν we denote $\nu_\infty = \infty$. Similarly, we denote by η_∞ the solution of $G(\nu_\infty, \eta) = 0$ and define $\eta_\infty = \infty$ if $\nu_\infty = \infty$. Note that for any $\nu \geq \nu_\infty$ $G(\nu, \eta_\infty) = 0$, hence for $\nu \geq \nu_\infty$, $I_0(\nu)$ remains empty, $I_-(\nu) = I_-(\nu_\infty)$, and $I_+(\nu) = I_+(\nu_\infty)$. We have thus characterized the form of the solution $0 \leq \nu \leq \nu_\infty$ through the equation $G(\nu, \eta) = 0$ which attains a unique zero at $\eta(\nu)$. Increasing ν beyond ν_∞ does not change the form of the solution (in terms of the partition into I_+ , I_- , I_0) hence we can confine the description of the relaxation path for ν to the interval $(0, \nu_\infty]$. In summary, the path $\eta(\nu)$ exists for any separable objective.

3. Geometry of the Relaxation Path

The previous section provided an abstract characterization of the relaxation path through the equation $G(\nu, \eta) = 0$. While the path can in principle be recovered for any individual value of ν by solving the equation $G(\nu, \eta) = 0$, we are interested in a computational feasible method for finding it entirely. This task may not be possible for general additively separable ϕ . Our main setting, the relaxed maximum entropy problem, is an example where the relaxation path $\nu \mapsto \eta(\nu)$ admits a simple geometric description. In Sec. 8 we discuss an additional case where the relaxation path admits a geometric description and a corresponding tracking scheme.

In the relaxed maximum entropy, the objective $\phi(\mathbf{p})$ is the relative entropy between the distribution $\mathbf{p} \in \Delta(\mathbf{m})$ and a *known* distribution $\mathbf{u} \in \Delta(\mathbf{m})$,

$$\phi(\mathbf{p}) = \sum_{j=1}^n m_j \phi_j(p_j) = \sum_{j=1}^n m_j p_j \log\left(\frac{p_j}{u_j}\right) .$$

The optimization problem is then

$$\begin{aligned} \min_{\mathbf{p} \in \Delta(\mathbf{m})} \quad & \sum_{j=1}^n m_j p_j \log\left(\frac{p_j}{u_j}\right) \\ \text{s.t.} \quad & \|\mathbf{p} - \mathbf{q}\|_\infty \leq 1/\nu . \end{aligned} \tag{13}$$

We refer to \mathbf{u} as the *prior* distribution and to \mathbf{q} as the *observed* distribution. (The term “prior distribution” is not used here in any Bayesian context.) It is assumed that $u_j > 0$ for $j = 1, \dots, n$. It is useful to examine the dual problem of (13), which can be shown to be

$$- \min_{\boldsymbol{\alpha}} \left\{ \log \left(\sum_{j=1}^n m_j u_j e^{\alpha_j} \right) - \sum_{j=1}^n m_j q_j \alpha_j + \frac{1}{\nu} \sum_{j=1}^n m_j |\alpha_j| \right\} . \tag{14}$$

Let Z denote the sum $\sum_{j=1}^n m_j u_j e^{\alpha_j}$. Given a solution for the dual problem, the primal solution \mathbf{p} can be reconstructed from $\boldsymbol{\alpha}$ as follows

$$p_j = \frac{u_j e^{\alpha_j}}{Z} . \tag{15}$$

Moreover, we can rewrite the dual objective in a mixed form using $\mathbf{p}(\boldsymbol{\alpha})$ as

$$- \sum_{j=1}^n m_j q_j \log(p_j(\boldsymbol{\alpha})) + \frac{1}{\nu} \sum_{j=1}^n m_j |\alpha_j| .$$

When $\mathbf{m} = \mathbf{1}$, the dual form amounts to finding an exponential tilt of the multinomial distribution \mathbf{u} , with an ℓ_1 penalty on the exponential tilt coefficients. Adding a constant term, the dual objective can be written in a mixed form as

$$D_{\text{KL}}(\mathbf{q} \parallel \mathbf{p}(\boldsymbol{\alpha})) + \frac{1}{\nu} \|\boldsymbol{\alpha}\|_1 .$$

As the ℓ_1 penalty tends to promote sparse solutions, the primal problem can be interpreted as the task of finding a *sparse exponential tilt*, namely, an exponential tilt \mathbf{p} of the prior distribution \mathbf{u} , in which $p_i \propto u_i$ for most $1 \leq i \leq n$, and which is close (in D_{KL}) to the observed distribution \mathbf{q} .

Building on these insights, we now turn to a geometric description of the relaxation path in this case. Our first step is to re-parameterize the problem by introducing a parameter $\mu = \nu e^{\eta+1}$. In terms of μ , equations (10) and (11) amount to

$$p_j = q_j + \frac{1}{\nu} \theta(\mu u_j - \nu q_j) \quad , \quad (16)$$

$$G(\nu, \mu) = \sum_{j=1}^n m_j \theta(\mu u_j - \nu q_j) = 0 \quad . \quad (17)$$

Before proceeding, we would like to point to an aesthetic symmetry. Note that (μ, \mathbf{u}) are interchangeable with (ν, \mathbf{q}) . We can thus swap the roles of the prior distribution with the observed distribution and obtain an analogous characterization.

In order to explore the dependency of μ on ν let us introduce the following sums

$$\mathcal{M} = \sum_{j \in I_+} m_j - \sum_{j \in I_-} m_j \quad , \quad \mathcal{U} = \sum_{j \in I_0} m_j u_j \quad , \quad \mathcal{Q} = \sum_{j \in I_0} m_j q_j \quad . \quad (18)$$

Fixing ν while using (18), we can rewrite (17) as

$$\mu \mathcal{U} - \nu \mathcal{Q} + \mathcal{M} = 0 \quad . \quad (19)$$

Clearly, so long as the partition of $[n]$ into the sets I_+, I_-, I_0 is intact, there is a simple linear relation between μ and ν . The number of possible subsets I_-, I_0, I_+ is finite. Thus, the range $0 < \nu < \infty$ decomposes into a finite number of intervals each of which corresponds to a fixed partition of $[n]$ into I_+, I_-, I_0 . Therefore, in each interval where I_0 is not empty, μ is a linear function of ν . Finally, recall that I_0 is not empty for $\nu < \nu_\infty$, where ν_∞ is given by (12), and empty for $\nu \geq \nu_\infty$.

To recap our derivation, the following lemma characterizes of the solution of $G(\nu, \cdot)$. We denote the relaxation path for μ with respect to ν by $\mu(\nu)$.

Lemma 2 *For $0 \leq \nu \leq \nu_\infty$, the value of μ as defined by (17) is unique. Further, the function $\mu(\nu)$ is a piecewise linear continuous function in ν . Increasing ν beyond ν_∞ does not change \mathbf{p} .*

This establishes the fact that $\mu(\nu)$ is a piecewise linear function. The lingering question is how many linear sub-intervals the function can attain. To study this property, we take a geometric view of the plane defined by (ν, μ) . Our combinatorial characterization of the number of sub-intervals makes use of the following definitions of lines in \mathbb{R}^2 ,

$$\ell_{+j} = \{(\nu, \mu) \mid u_j \mu - q_j \nu = +1\} \quad (20)$$

$$\ell_{-j} = \{(\nu, \mu) \mid u_j \mu - q_j \nu = -1\} \quad (21)$$

$$\ell_0 = \{(\nu, \mu) \mid \mu \mathcal{U} - \nu \mathcal{Q} + \mathcal{M} = 0\} \quad , \quad (22)$$

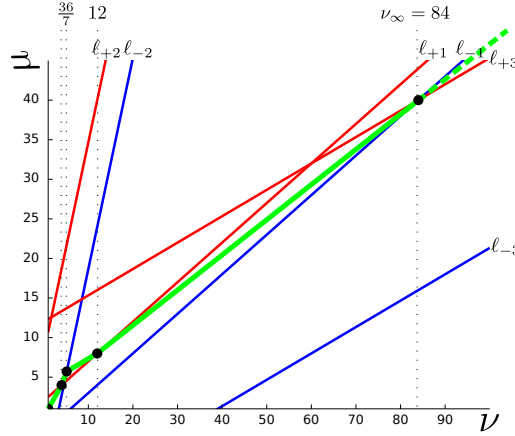


Figure 2: An illustration of the function $\mu(\nu)$ for a synthetic 3 dimensional example.

where $-\infty < \nu < \infty$ and $j \in [n]$. The next theorem gives an upper bound on the number of linear segments the function $\mu(\cdot)$ may attain. While the bound is quadratic in the dimension, for both artificial data and real datasets the bound is too pessimistic, as we demonstrate in the sequel.

Theorem 3 *The piecewise linear function $\mu(\nu)$ consists of at most n^2 linear segments for $\nu \in \mathbb{R}_+$.*

Proof Since we showed that $\mu(\nu)$ is a piecewise linear function, it remains to show that it has at most n^2 linear segments. Consider the two dimensional function $G(\nu, \mu)$ from (17). The (ν, μ) plane is divided by the $2n$ straight lines $\ell_1, \ell_2, \dots, \ell_n, \ell_{-1}, \ell_{-2}, \dots, \ell_{-n}$ into at most $2n^2 + 1$ polygons. The latter property is proved by induction. It clearly holds for $n = 0$. Assume that it holds for $n - 1$. Line ℓ_n intersects the previous $2n - 2$ lines in at most $2n - 2$ points, thus splitting at most $2n - 1$ polygons into two separate polygonal parts. Line ℓ_{-n} is parallel to ℓ_n , again adding at most $2n - 1$ polygons. Together we get at most $2(n - 1)^2 + 1 + 2(2n - 1) = 2n^2 + 1$ polygons, as required per induction. Recall that $\mu(\nu)$ is linear inside each polygon. The two extreme polygons where $G(\nu, \mu) = \pm n$ clearly disallow $G(\nu, \mu) = 0$, hence $\mu(\nu)$ can have at most $2n^2 - 1$ segments for $-\infty < \nu < \infty$. Lastly, we use the symmetry $G(-\nu, -\mu) = -G(\nu, \mu)$ which implies that for $\nu \in \mathbb{R}_+$ we have at most n^2 segments, as required. \blacksquare

When the prior \mathbf{u} is uniform, i.e. $u_j = 1/\sum_j m_j$ for all $j \in [n]$, the number of segments is at most $n + 1$. We defer the analysis of the uniform case to a later section as the proof stems from the algorithms we describe in the sequel.

To conclude this section, we characterize the path $\mu(\nu)$ in the following toy example. Let $\mathbf{u} = (1/2, 1/8, 1/12)$, $\mathbf{q} = (1/4, 1/3, 1/36)$, and $\mathbf{m} = (1, 2, 3)$. Note that

$\mathbf{u} \cdot \mathbf{m} = \mathbf{q} \cdot \mathbf{m} = 1$ as required from our definition of distributions with multiplicity. The complete characterization of $\mu(\nu)$ for $0 < \nu < \infty$ is as follows,

region of ν	I_-	I_0	I_+	$\mu(\nu)$
$0 < \nu < 4$	$\{\}$	$\{1, 2, 3\}$	$\{\}$	$\mu = \nu$
$4 \leq \nu < \frac{36}{7}$	$\{\}$	$\{2, 3\}$	$\{1\}$	$\mu = 4 + \frac{3}{2}(\nu - 4)$
$\frac{36}{7} \leq \nu < 12$	$\{2\}$	$\{3\}$	$\{1\}$	$\mu = \frac{40}{7} + \frac{1}{3}(\nu - \frac{36}{7})$
$12 \leq \nu < 84$	$\{2\}$	$\{1, 3\}$	$\{\}$	$\mu = 8 + \frac{4}{9}(\nu - 12)$
$\nu_\infty = 84 \leq \nu$	$\{1, 2\}$	$\{\}$	$\{3\}$	$\mu = 8 + \frac{4}{9}(\nu - 12)$

The above table implies that $\nu_\infty = 84$ and $\mu_\infty = 40$. Thus, the partition $I_- = \{1, 2\}$, $I_+ = \{3\}$, and I_0 is empty remains intact for any $\nu \geq 84$. Figure 2 shows the constraint lines $\ell_{\pm 1}, \ell_{\pm 2}, \ell_{\pm 3}$, the path segments and the path itself. Interestingly, note that the cardinalities of I_0 and I_+ are not monotone. Indeed, the first coordinate enters I_+ from I_0 and then returns to I_0 , finally ending at I_- for $\nu \geq \nu_\infty$. This kind of non-monotone behavior is the reason why $O(n^2)$ linear segments are necessary to describe $\mu(\nu)$ in the worst case.

4. Path Tracking Algorithms

In this section we build on the geometric description above and discuss algorithms for tracking the maximum entropy relaxation path. The algorithms are based on a local search for the next intersection of the line ℓ_0 with one of the lines $\ell_{\pm j}$. These algorithms are simple to implement and efficient in practical settings. In Appendix A we outline a more complicated algorithm with slightly better worst case performance, which maintains global information of the homotopy. Discussion of the global tracking algorithm is deferred to the appendix as it is not straightforward to implement.

4.1 Local Homotopy Tracking

Since we showed that the optimal solution \mathbf{p} can be straightforwardly obtained from the variable μ , it suffices to devise an algorithm that efficiently tracks the function $\mu(\nu)$ as we traverse the plane (ν, μ) from $\nu = 0$ through the last change point which we denoted as (ν_∞, μ_∞) . In this section we give an algorithm that traces $\mu(\nu)$ by tracking the changes in $\mu(\nu)$ through a local search process. Concretely, we start by computing the initial slope of ℓ_0 at $\nu = 0$. We then find the closest intersection with a line ℓ_j (for $1 \leq |j| \leq n$) and calculate the new slope of ℓ_0 as the intersection with the line induces a new partition into the sets I_+, I_-, I_0 . We continue this process until we reach the point (ν_∞, μ_∞) beyond which the partition into (I_\pm, I_0) does not change.

More formally, the local tracking algorithm follows the piecewise linear function $\mu(\nu)$, segment by segment. Each segment corresponds to a subset of the line ℓ_0 for a *given* triplet $(\mathcal{M}, \mathcal{U}, \mathcal{Q})$. It is simple to show that $\mu(0) = 0$, hence we start with $(\nu, \mu) = (0, 0)$. Given the pair (ν, μ) the partition into the sets I_\pm and I_0 is

straightforward as we can rewrite (3) as,

$$\begin{aligned} I_+ &= \{1 \leq j \leq n \mid \mu u_j - \nu q_j \geq 1\} \\ I_0 &= \{1 \leq j \leq n \mid |\mu u_j - \nu q_j| < 1\} \\ I_- &= \{1 \leq j \leq n \mid \mu u_j - \nu q_j \leq -1\} . \end{aligned}$$

This form of index partitioning implies that given (ν, μ) we can calculate $\mathcal{M}, \mathcal{U}, \mathcal{Q}$ directly as follows,

$$\mathcal{M} = \sum_{\mu u_j - \nu q_j \geq 1} m_j - \sum_{\mu u_j - \nu q_j \leq -1} m_j \quad \mathcal{U} = \sum_{|\mu u_j - \nu q_j| < 1} m_j u_j \quad \mathcal{Q} = \sum_{|\mu u_j - \nu q_j| < 1} m_j q_j . \quad (23)$$

From the triplet $(\mathcal{M}, \mathcal{U}, \mathcal{Q})$ the initial characterization of ℓ_0 is readily available as we can write,

$$\mu = \frac{\nu \mathcal{Q} - \mathcal{M}}{\mathcal{U}} = \frac{\mathcal{Q}}{\mathcal{U}} \nu - \frac{\mathcal{M}}{\mathcal{U}} . \quad (24)$$

In words, the line ℓ_0 has a slope of \mathcal{Q}/\mathcal{U} and an intercept of $-\mathcal{M}/\mathcal{U}$. Initially the set $I_0 = [n]$, $\mathcal{M} = 0$, and therefore $\mathcal{Q} = \mathcal{U} = 1$, which implies that the initial slope of ℓ_0 is 1 and the intercept is 0. We now track the value of μ as ν increases (and the original relaxation parameter δ decreases). The characterization of the line ℓ_0 remains intact until ℓ_0 hits one of the lines ℓ_j for $1 \leq |j| \leq n$. To find the line intersecting ℓ_0 we need to compute the potential intersection points (μ_j, ν_j) for $\nu_{-n}, \nu_{-n+1}, \dots, \nu_{-1}, \nu_1, \nu_2, \dots, \nu_n$ where $(\nu_j, \mu_j) = \ell_0 \cap \ell_j$. This amounts to calculating the potential intersection values,

$$\nu_j = \frac{\mathcal{M} u_{|j|} + \mathcal{U} \cdot \text{sign}(j)}{\mathcal{Q} u_{|j|} - \mathcal{U} q_{|j|}} \quad ; \quad \text{sign}(j) = \begin{cases} 1 & j > 0 \\ -1 & j < 0 \end{cases} . \quad (25)$$

The lines for which the denominator is zero correspond to an infeasible intersection and can be discarded. The smallest value ν_j which is larger than the current recorded value of ν (i.e. the last observed intersection of ℓ_0 with one the lines ℓ_j) corresponds to the next line intersecting ℓ_0 . From ν_j we compute μ_j using (24). We now can construct the next segment of ℓ_0 , which starts at (ν_j, μ_j) by calculating a new value for the triplet $(\mathcal{M}, \mathcal{U}, \mathcal{Q})$ as prescribed by (23). The homotopy tracking process finishes once we cannot find any pair (ν_j, μ_j) for which ν_j is greater than the most recently traced found for μ . That is, the last intersection that was found corresponds to (ν_∞, μ_∞) .

In the above description of the local tracking algorithm, the formation of the sets I_\pm and I_0 is tacit. Moreover, calculating the sums \mathcal{M}, \mathcal{Q} , and \mathcal{U} from scratch upon every newly found intersection of ℓ_0 with ℓ_j is not mandatory since each such intersection corresponds to moving a *single* constraint $|p_j - q_j| \leq 1/\nu$ from I_\pm to I_0 or vice versa. By explicitly tracking the set I_+, I_- , and I_0 as they change, we can update the sums \mathcal{M}, \mathcal{Q} , and \mathcal{U} in a constant time upon each newly encountered

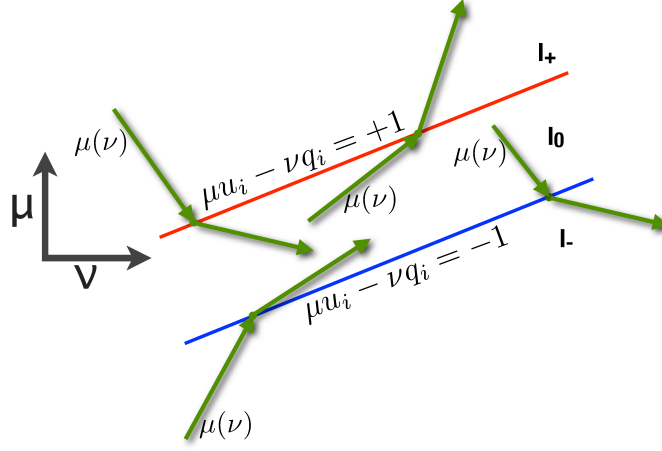


Figure 3: Illustration of the possible intersections between $\mu(\nu)$ and ℓ_j and the corresponding transition between the sets I_{\pm}, I_0 .

intersection. We therefore present an equivalent, yet more efficient, procedure in which the sets \mathcal{M} , \mathcal{Q} , and \mathcal{U} are updated incrementally. Further, we use the latter property and the more elaborate tracking scheme in the next section in which we analyze the case where the prior distribution \mathbf{u} is uniform. As before, our goal is to track the piecewise linear function $\mu(\nu)$, segment by segment where each segment forms a straight line $\ell_0(\mathcal{M}, \mathcal{U}, \mathcal{Q})$. In the alternative view, we track the sets I_-, I_0, I_+ by defining an auxiliary variable per coordinate. Given the current partition of $[n]$ into sets we denote,

$$s_j = \begin{cases} -1 & j \in I_- \\ 0 & j \in I_0 \\ +1 & j \in I_+ \end{cases} . \quad (26)$$

As in the tacit version, the explicit version starts with $(\nu, \mu) = (0, 0)$, $\mathcal{M} = 0$, and $\mathcal{U} = \mathcal{Q} = 1$. Identically, on each step we compute the $2n$ intersection values $(\nu_j, \mu_j) = \ell_0 \cap \ell_j$ for $1 \leq |j| \leq n$ and find the nearest intersection. However, at this point the two procedures depart. Rather than tacitly deferring the identification of the type of intersection to the computation of the new sums, we explicitly characterize the form of the change in the sets I_{\pm} and I_0 due to the newly found intersection. Recall that $\frac{\mathcal{Q}}{\mathcal{U}}$ is the left slope of $\mu(\nu)$ as represented by the current line segment ℓ_0 . The slope of ℓ_j is $\frac{q_{|j|}}{u_{|j|}}$. Thus, when $\frac{\mathcal{Q}}{\mathcal{U}} > \frac{q_{|j|}}{u_{|j|}}$ the $|j|$ 'th constraint is moving “up” from I_- to I_0 or from I_0 to I_+ . When $\frac{\mathcal{Q}}{\mathcal{U}} < \frac{q_{|j|}}{u_{|j|}}$ the $|j|$ 'th constraint is moving “down” from I_+ to I_0 or from I_0 to I_- . See also Fig. 4 for an illustration of the possible transitions between the sets. For instance, the slope of $\mu(\nu)$ on the bottom left part of the figure is larger than the slope the line it intersects. Since this line defines the boundary between I_- and I_0 , we transition from I_- to I_0 . All four possible transitions

Algorithm 1 The local tracking algorithm for relaxed maximum entropy.

```

1: input: Distributions  $\mathbf{q}, \mathbf{u}$  ; Multiplicity:  $\mathbf{m}$ 
2: initialize:  $\mathcal{Q} = \mathcal{U} = 1$ ,  $\mathcal{M} = 0$ ,  $L = \{(0, 0)\}$ ,  $\nu_{last} = 0$ ,  $\forall j \in [n] : s_j = 0$ 
3: while  $\exists j$  s.t.  $s_j = 0$  do
4:    $\nu_c = \infty$ 
5:   for all  $j \in \{-n, \dots, -1, 1, \dots, n\}$  do
6:     if  $(\mathcal{Q}u_{|j|} - \mathcal{U}q_{|j|})s_j \leq 0$  then
7:        $\nu = \frac{\mathcal{M}u_{|j|} + \mathcal{U}\text{sign}(j)}{\mathcal{Q}u_{|j|} - \mathcal{U}q_{|j|}}$ 
8:       if  $\nu < \nu_c$  then
9:          $\nu_c \leftarrow \nu; j_c \leftarrow j$ 
10:      end if
11:    end if
12:  end for
13:  if  $\nu_c = \infty$  then
14:    break
15:  end if
16:   $\mu_c = \frac{\nu_c \mathcal{Q} - \mathcal{M}}{\mathcal{U}}$  ;  $L \leftarrow L \cup \{(\nu_c, \mu_c)\}$ 
17:   $s_{|j_c|} \leftarrow s_{|j_c|} + \text{sign}(\mathcal{Q}u_{|j_c|} - \mathcal{U}q_{|j_c|})$ 
18:   $\mathcal{M} \leftarrow \mathcal{M} + \text{sign}(\mathcal{Q}u_{|j_c|} - \mathcal{U}q_{|j_c|}) m_{|j_c|}$ 
19:   $\mathcal{U} \leftarrow \mathcal{U} + \text{sign}(j_c) \text{sign}(\mathcal{Q}u_{|j_c|} - \mathcal{U}q_{|j_c|}) m_{|j_c|} u_{|j_c|}$ 
20:   $\mathcal{Q} \leftarrow \mathcal{Q} + \text{sign}(j_c) \text{sign}(\mathcal{Q}u_{|j_c|} - \mathcal{U}q_{|j_c|}) m_{|j_c|} q_{|j_c|}$ 
21: end while
22: return  $L$ 

```

are depicted in the figure. Thus, we need to consider only indices j such that (25) is defined and

$$(\mathcal{Q}u_{|j|} - \mathcal{U}q_{|j|}) s_{|j|} \leq 0 . \quad (27)$$

Again, let ν_j be the smallest intersection value satisfying (27). If there is no such value, we are done with the homotopy tracking process. Otherwise, we can now update the sums \mathcal{M} , \mathcal{Q} and \mathcal{U} based on the single transition of the j 'th element between the characteristic sets. We also need to update s_j itself. By isolating the j 'th term in (23), the update of all the sums and s_j now takes the following incremental form,

$$\begin{aligned}
s_{|j|} &\leftarrow s_{|j|} + \text{sign}(\mathcal{Q}u_{|j|} - \mathcal{U}q_{|j|}) \\
\mathcal{M} &\leftarrow \mathcal{M} + \text{sign}(\mathcal{Q}u_{|j|} - \mathcal{U}q_{|j|}) m_{|j|} \\
\mathcal{U} &\leftarrow \mathcal{U} + \text{sign}(j) \text{sign}(\mathcal{Q}u_{|j|} - \mathcal{U}q_{|j|}) m_{|j|} u_{|j|} \\
\mathcal{Q} &\leftarrow \mathcal{Q} + \text{sign}(j) \text{sign}(\mathcal{Q}u_{|j|} - \mathcal{U}q_{|j|}) m_{|j|} q_{|j|} .
\end{aligned}$$

We are done with the tracking process when I_0 is empty, i.e. for all j $s_j \neq 0$. The pseudo code of the entire process is provided in Algorithm 1.

Complexity. The local tracking algorithm requires $O(n)$ memory and $O(n\kappa)$ operations where κ is the number of change points in the function $\mu(\nu)$. When κ is relatively small, this algorithm is simple and efficient to implement. In Appendix A we give a more complicated algorithm, which employs an auxiliary priority queues and requires fewer number of operations when $\kappa > n \log(n)$. A illustration of the tracking result, $\mu(\nu)$, along with the lines $\ell_{\pm j}$, that provide a geometrical description of the problem, is given in Fig. 2.

4.2 Fast Homotopy Tracking for Sparse Observations

In numerous practical settings, while the dimension n may be very large, the number of zero entries in \mathbf{q} can be substantial. We now discuss an improvement to the local tracking algorithm that renders its feasible for very large dimension n so long as \mathbf{q} is sparse. Let us denote by s the support of \mathbf{q} , $s := |\{1 \leq j \leq n \mid q_j \neq 0\}|$,

Recall that the principle underlying the local tracking algorithm is that every coordinate j induces two lines in the (ν, μ) plane, denoted $\ell_{\pm j}$ as given by (20) and (21). A coordinate for which $q_j = 0$ corresponds to a *horizontal* line $\ell_{\pm j}$ described by the equation by $u_j \mu = \pm 1$. Since the path $\mu(\nu)$ is non-decreasing with $\mu(0) = 0$, each horizontal line ℓ_{-j} resides outside the positive quadrant in (ν, μ) plane and is never intersected. Further, each of the lines ℓ_{+j} is intersected exactly once. Note that $u_j > u_k$ implies that the line ℓ_{+j} is intersected at $\mu = \frac{1}{u_j}$, before the line ℓ_{+k} , whose intersection is at $\mu = \frac{1}{u_k}$. Therefore, we sort the values $\{u_j \mid q_j = 0\}$ in decreasing order, as a preliminary step. Then, the search for the next intersection in the local tracking algorithm can be confined to scanning $2s + 1$ lines only. Namely, the $2s$ lines corresponding to nonzero values of \mathbf{q} and the next horizontal line to be intersected from the zero set of \mathbf{q} .

Figure 4 provides an illustration of the constraint lines and the path in the (ν, μ) plane when \mathbf{q} is sparse. In this 8-dimensional toy example for sparse observations, $\mathbf{u} = (0.0372, 0.0445, 0.0403, 0.0144, 0.0268, 0.0088, 0.0389, 0.0390)$ is a vector whose entries were sampled from a uniform distribution on $[0, 1]$ and normalized, $\mathbf{q} = (0, \frac{5}{8}, 0, 0, 0, 0, \frac{3}{8}, 0)$, and $\mathbf{m} = (0, 10, 0, 0, 0, 0, 10, 0)$. Observe that each coordinate where $q_j = 0$ donates a single horizontal line, and that these lines are intersected according to the order of the corresponding values u_j .

This fast version of the local tracking algorithm requires $O(n)$ memory and $O(n \log n + s\kappa)$ operations where κ is the number of path change points. From Theorem 3 we have in this case $\kappa \leq s^2 + n$ so that the worst case time complexity of the fast algorithm is $O(n \log n + sn + s^3)$. Therefore, in the practical case where the sparsity s of the observed distribution is logarithmic in the dimension the total complexity even in the worst case becomes $O(n \log n)$, which makes the algorithm practical for very high dimensional problems.

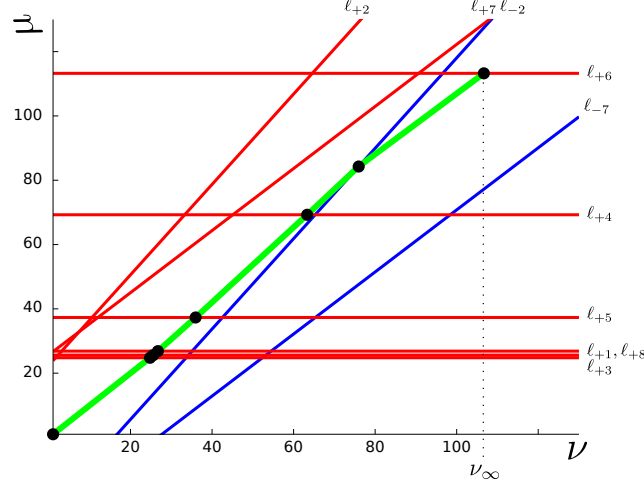


Figure 4: The relaxation path for a toy 8-dimensional example with a 2-sparse observations vector – intersects mostly horizontal constraint lines

4.3 Fast Homotopy Tracking for Uniform Prior

We chose to denote the prior distribution by \mathbf{u} to underscore the fact that in the case of no prior knowledge \mathbf{u} is the *uniform* distribution. When the prior is uniform, then for all $j \in [n]$ the value of u_j is the same and is equal to

$$u_0 \stackrel{\text{def}}{=} \left(\sum_{j=1}^n m_j \right)^{-1} .$$

Moreover, for a uniform prior objective function amounts to the negative entropy. By reversing the sign of the objective, we obtain the classical maximum entropy problem. Similarly to the case of sparse observed vector, the case of a uniform prior distribution simplifies the geometry and consequently significantly lowers the complexity of the tracking algorithm.

Let us consider a point (ν, μ) on the boundary between I_0 and I_+ , namely, there exists a line ℓ_{+i} such that,

$$\mu u_i - \nu q_i = \mu u_0 - \nu q_i = 1 \quad .$$

By definition, for any $j \in I_0$ we have

$$\mu u_j - \nu q_j = \mu u_0 - \nu q_j < 1 = \mu u_0 - \nu q_i \quad .$$

Thus, $q_i < q_j$ when $i \in I_+$ and for all $j \in I_0$. The inequality implies that

$$m_j u_0 q_j > m_j u_0 q_i \quad . \tag{28}$$

Summing (28) over $j \in I_0$ we get that

$$\mathcal{Q} u_0 = \sum_{j \in I_0} m_j q_j u_0 > \sum_{j \in I_0} m_j u_0 q_i = \mathcal{U} q_i ,$$

hence,

$$\frac{q_i}{u_i} = \frac{q_i}{u_0} < \frac{\mathcal{Q}}{\mathcal{U}}$$

and we must be moving “up” from I_0 to I_+ when the line ℓ_0 hits a line ℓ_i . Similarly we must be moving “down” from when ℓ_0 intersects a line on the boundary between I_0 and I_- . We summarize these properties in the following theorem. Here, we say that the set $I(\nu)$ is *monotonically non-decreasing* if $i \in I(\nu)$ implies $i \in I(\nu_1)$ whenever $\nu \leq \nu_1$.

Theorem 4 *When the prior distribution \mathbf{u} is uniform, $I_-(\nu)$ and $I_+(\nu)$ are monotonically nondecreasing and $I_0(\nu)$ is monotonically non-increasing in $\nu > 0$. Further, the piecewise linear function $\mu(\nu)$ consists of at most $n + 1$ line segments.*

The local tracking algorithm when the prior is uniform is particularly simple and efficient. Intuitively, there is a single condition which controls the order in which indices enter I_{\pm} from I_0 , which is simply how “far” each q_j is from u_0 , the single prior value. Therefore, the algorithm starts by sorting \mathbf{q} . Let $q_{\pi_1} > q_{\pi_2} > \dots > q_{\pi_n}$ denote the sorted vector. Instead of maintaining a vector of set-indicators \mathbf{s} , we merely maintain two indices which denote as j_- and j_+ . These indices designate the size of I_- and I_+ that were constructed thus far. Due to the monotonicity property of the sets I_{\pm} , as ν grows, the two sets can be written as,

$$I_- = \{\pi_j \mid 1 \leq j < j_-\} \quad \text{and} \quad I_+ = \{\pi_j \mid j_+ < j \leq n\} .$$

The local tracking algorithm starts as before with $\nu = 0$, $\mathcal{M} = 0$, $\mathcal{U} = \mathcal{Q} = 1$. We also set $j_- = 1$ and $j_+ = n$ which by definition imply that I_+ and I_- are empty, and $I_0 = [n]$. On each iteration we need to compare only two values which we compactly denote as,

$$\nu_{\pm} = \frac{\mathcal{M} u_0 \pm \mathcal{U}}{\mathcal{Q} u_0 - \mathcal{U} q_{\pi_{j_{\pm}}}} .$$

When $\nu_- \leq \nu_+$ we encounter a transition from I_0 to I_- and as we encroach I_- we perform the update

$$\begin{aligned} \nu &\leftarrow \nu_- \\ \mathcal{M} &\leftarrow \mathcal{M} - m_{\pi_{j_-}} \\ \mathcal{U} &\leftarrow \mathcal{U} - m_{\pi_{j_-}} u_0 \\ \mathcal{Q} &\leftarrow \mathcal{Q} - m_{\pi_{j_-}} q_{\pi_{j_-}} \\ j_- &\leftarrow j_- + 1 . \end{aligned}$$

Similarly when $\nu_- > \nu_+$ we perform the update

$$\begin{aligned}\nu &\leftarrow \nu_+ \\ \mathcal{M} &\leftarrow \mathcal{M} + m_{\pi_{j_+}} \\ \mathcal{U} &\leftarrow \mathcal{U} - m_{\pi_{j_+}} \mathbf{u}_0 \\ \mathcal{Q} &\leftarrow \mathcal{Q} - m_{\pi_{j_+}} q_{\pi_{j_+}} \\ j_+ &\leftarrow j_+ - 1 \ .\end{aligned}$$

The local tracking algorithm stops when $j_- > j_+$ as we exhausted the transitions out of the set I_0 , which becomes empty. We have thus shown that the local tracking algorithm for a uniform prior requires $O(n)$ memory and $O(n \log(n))$ operations.

5. Model Selection Along the Relaxation Path

In this section we study the following attractive property of the relaxed maximum entropy problem. Suppose that we evaluate models by their likelihood on a held-out validation set. As we will see, there is a unique admissible model for each possible model size. Equivalently, in terms of our geometric description of the relaxation path, there is only one admissible relaxation parameter per path interval. Moreover, this discrete family of possible relaxation parameters can be recovered efficiently to arbitrary precision, without performing a grid search over the ν variable.

Setup. Once the maximum entropy problem (13) is solved, the distribution \mathbf{p} is efficiently characterized for each possible relaxation value ν . Assume that we have calculated the relaxation path for given vectors \mathbf{u} and \mathbf{q} . To make the dependence on ν explicit, we write $\mathbf{p}(\nu)$ for the primal solution corresponding to the relaxation parameter ν . Having solved for the entire relaxation path, we can evaluate the map $\nu \mapsto \mathbf{p}(\nu)$ at any $\nu \geq 0$. This allows us the luxury of having all possible values of ν to choose from.

Assume that we have available validation data in the form of a vector of counts, $\mathbf{r} \in \mathbb{N}^n$. (We can normalize \mathbf{r} to be in the probability simplex without changing the value of the optimal solution.) To choose ν , we minimize w.r.t. ν the negative empirical log-likelihood for the validation data, $-\sum_i r_i \log p_i(\nu)$. As we will shortly see, this minimization is easiest to handle when the optimization parameter is the *inverse* of the relaxation parameter ν we have used so far, denoted by $\lambda = \frac{1}{\nu}$. We thus need to solve the problem

$$\lambda^* = \arg \min_{0 \leq \lambda \leq 1} L_r(\lambda) \stackrel{\text{def}}{=} - \sum_j r_j \log p_j(\lambda) \ .$$

Efficient minimization of the validation likelihood on each path segment.

Using λ , it is convenient to express the primal solution (11) as follows,

$$p_j(\lambda) = \begin{cases} q_j + \lambda & j \in I_+ \\ u_j \mu \lambda & j \in I_0 \\ q_j - \lambda & j \in I_- \end{cases} , \quad (29)$$

where I_{\pm} and I_0 are given by (3) and depend on ν (or, equivalently, on λ). We can thus write the objective $L_{\mathbf{r}}(\lambda)$ as

$$- \sum_{j \in I_+} r_j \log(q_j + \lambda) - \sum_{j \in I_-} r_j \log(q_j - \lambda) - \sum_{j \in I_0} r_j \log(u_j \mu \lambda) . \quad (30)$$

Since the terms u_i does not depend on λ , they can be omitted from $L_{\mathbf{r}}(\lambda)$ without changing the minimizer, so that the last term can be replace with $-\sum_{j \in I_0} r_j \log(\mu \lambda)$. Let us now examine the product $\mu \lambda = \mu/\nu$. The latter ratio is constant between path change points, and satisfies (19) which implies that

$$\frac{\mu}{\nu} = \frac{\mathcal{Q} - \mathcal{M}/\nu}{\mathcal{U}} = \frac{\mathcal{Q} - \mathcal{M}\lambda}{\mathcal{U}} .$$

We can further omit the constant \mathcal{U} and replace the last term in $L_{\mathbf{r}}(\lambda)$ with

$$- \sum_{j \in I_0} r_j \log(\mathcal{Q} - \mathcal{M}\lambda)$$

without changing the minimizer. To recap, between each consecutive points $(1/\nu_{i+1}, 1/\nu_i)$ the validation set likelihood, up to constant terms, is equal to,

$$L_{\mathbf{r}}(\lambda) = - \sum_{j \in I_+} r_j \log(q_j + \lambda) - \sum_{j \in I_-} r_j \log(q_j - \lambda) - \sum_{j \in I_0} r_j \log(\mathcal{Q} - \mathcal{M}\lambda) .$$

It is easy to check that the second order derivative of $L_{\mathbf{r}}(\lambda)$ is positive, namely, it is convex. To recap, we have the following simple picture. While the validation objective we wish to minimize over $[0, 1]$ is not convex, it is piecewise convex: specifically, it is convex on any interval where $\nu \mapsto \mu(\nu)$ is linear, namely between any two path change points, where the sets I_{\pm}, I_0 are constant. See also Fig. 5.

It remains to show how to find the optimum in each interval numerically. Concretely, for every consecutive path change points $\nu_i < \nu_{i+1}$ we wish to solve

$$\min_{\frac{1}{\nu_{i+1}} \leq \lambda \leq \frac{1}{\nu_i}} L_{\mathbf{r}}(\lambda) = - \sum_{j \in I_+} r_j \log(q_j + \lambda) - \sum_{j \in I_-} r_j \log(q_j - \lambda) - \sum_{j \in I_0} r_j \log(\mathcal{Q} - \mathcal{M}\lambda) .$$

Since the objective $L_{\mathbf{r}}(\lambda)$ is convex on a real interval, the minimum exists, is unique, and can be found by bisection. In each interval, we search for the λ for which

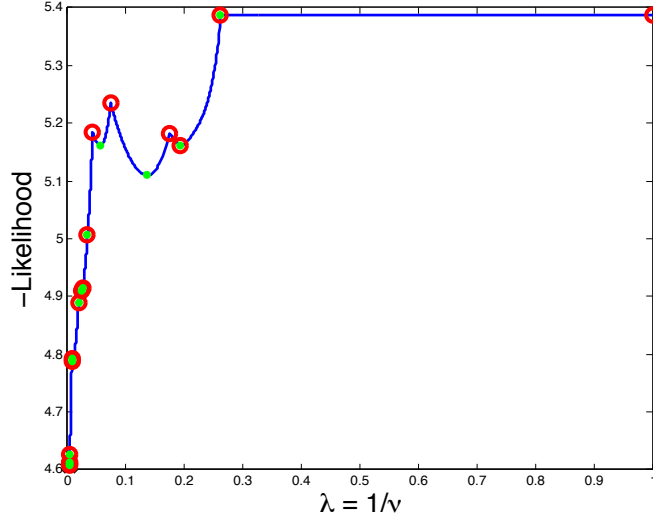


Figure 5: The validation set likelihood is a piecewise convex function (Red: path nodes, green: minimum in each path segment)

$\frac{d}{d\lambda} L_{\mathbf{r}}(\lambda) = 0$. The derivative of $L_{\mathbf{r}}(\lambda)$

$$L'_{\mathbf{r}}(\lambda) = - \sum_{j \in I_+} r_j \frac{r_j}{q_j + \lambda} + \sum_{j \in I_-} r_j \frac{r_j}{q_j - \lambda} + \left(\frac{\mathcal{M}}{\mathcal{Q} - \mathcal{M}\lambda} \right) \sum_{j \in I_0} r_j ,$$

is an increasing function in λ . Thus we simply need to search by bisection for the zero crossing of $\frac{d}{d\lambda} L_{\mathbf{r}}$.

A discrete set of admissible models. We have thus revealed a simple and aesthetic trade-off between model complexity and validation loss for the relaxed maximum entropy problem. Having solved for the path $\nu \mapsto \mu(\nu)$, we obtain a collection of intervals, on each of which the path is linear. In each interval, the support of the dual variable α is constant. The support size that is thus associated with each path interval represents the number of entries in which the solution \mathbf{p} is not proportional to the base distribution \mathbf{u} , or in other words, the model complexity. After finding the minimum cross-validation loss at each interval, we can further associate with each path interval a single validation loss $L_{\mathbf{r}}(\nu^*)$ (the validation loss minimum over that interval) and a single value ν^* (where this minimum is obtained). We thus obtain a discrete list of possible models, where each model is expressed by its size, a regularization value, and a validation likelihood.

Since increasing model complexity only makes sense if it reduces the validation loss, we can cull the list and keep only the options where the validation loss decreases with the increase in the support of α . Further, we need only consider the cases where the support of α ranges from 0 (where the regularization penalty is infinite

$\text{supp}(\boldsymbol{\alpha})$	ν^*	$L_{\mathbf{r}}^*$
0	$\nu_0^* = 1$	$L_{\mathbf{r}}^*(1)$
1	ν_1^*	$L_{\mathbf{r}}^*(\nu_1^*)$
\vdots	\vdots	\vdots
k	ν_k^*	$L_{\mathbf{r}}^*(\nu_k^*)$

Table 1: An illustration of the discrete list of possible parameters for a relaxed maximum entropy problem, given a validation set.

and $\mathbf{p} = \mathbf{u}$) to the model complexity that globally minimizes the validation loss. Formally, we obtain table of the form of Table 1 which contains an increasing list $\nu_0^* = 1 < \nu_1^* < \dots < \nu_k^*$ such that $\nu_k^* = \arg\min_{\nu \geq 1} L_{\mathbf{r}}(\nu)$, and such that for each $j = 0, \dots, k$,

$$\nu_j^* = \arg \min_{\nu : \text{supp}(\boldsymbol{\alpha}(\nu))=j} L_{\mathbf{r}}(\nu),$$

where $\boldsymbol{\alpha}(\nu)$ is the dual solution of $\mathbf{p}(\nu)$ and $\text{supp}(\boldsymbol{\alpha}(\nu))$ is the number of non-zero values in $\boldsymbol{\alpha}$.

6. Empirical Complexity of the Relaxation Path

In this section we assess the empirical complexity of the relaxation path, in terms of number of path nodes. As we will show, in practice, the number of change points is close to linear in the dimension. This renders the local tracking algorithms viable approaches for real datasets. We consider two examples, one with synthetic data and the other with data from natural text. It is worth noting though that we obtained qualitatively similar results in all of our experiments.

In the first experiment the prior distribution \mathbf{u} was a Zipf distribution of the form $u_j \sim \frac{1}{2+j}$. The observed distribution \mathbf{q} was sampled from a Zipf distribution which we denote by $\bar{\mathbf{q}}$ where $\bar{q}_j \sim \frac{1}{j}$. The dimension was set to 50,000 and we normalized \mathbf{u} , $\bar{\mathbf{q}}$, and the sampled distribution \mathbf{q} so that they sum to 1. We generated numerous observed distributions \mathbf{q} by sampling from $\bar{\mathbf{q}}$. For each sample size we generated 10 distributions from $\bar{\mathbf{q}}$ and ran the local tracking algorithm with \mathbf{u} and the sampled distribution \mathbf{q} . We then computed the mean over the 10 runs of the relaxation path complexity. Since the samples varied in size, \mathbf{q} tended to have more zero entries the smaller the sample size was. In Fig. 6 we show the relaxation path complexity in terms of the number of changes points, divided by the dimension, as a function of the sample size (also divided by the dimension). Evidently, the relaxation path complexity grows almost linearly as a function of the sample sizes we examined. We also checked the complexity without sampling by setting $\mathbf{q} = \bar{\mathbf{q}}$. The last point on the graph, which we kept disconnected, designates the complexity when using $\bar{\mathbf{q}}$ as

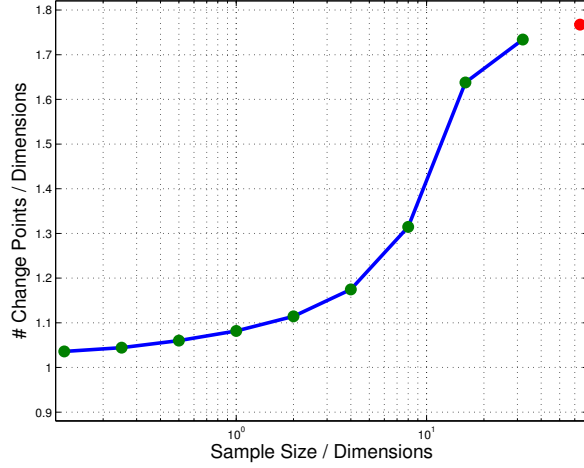


Figure 6: Homotopy complexity as a function of the sample size.

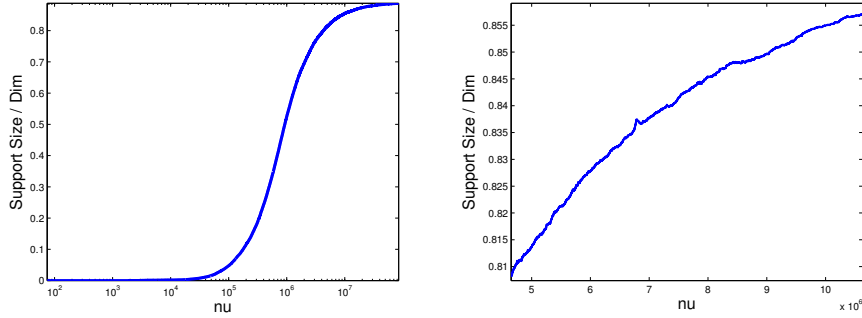


Figure 7: The cardinality of $I_+ \cup I_-$ as a function of ν . Right: a zoomed in look into the middle range.

the observed distribution. It is clear that for much larger samples the complexity asymptotes at less than $1.8n$. In fact, we never observed complexity above $2n$ in our experiments with Zipf distributions.

In the second experiment we used the Reuters Corpus Volume 1 (RCV1). The RCV1 dataset consists of a collection of approximately 800,000 text articles, each of which is assigned multiple labels. There are 4 high-level categories, Economics, Commerce, Medical, and Government (ECAT, CCAT, MCAT, GCAT), and multiple more specific categories. After stemming and stop-listing we obtained a dictionary of 17,632 words for the entire collection. We used the maximum likelihood estimate of the entire collection to define the prior distribution and the collection resulting by taking a single category as the observed distribution. This setting mimics the source adaptation setting of (Blitzer et al., 2007) in which we need to adapt a distribution derived from a large collection to a concrete distribution. In Fig. 7 we show the size

of the support, i.e. $|I_+ \cup I_-|$ as a function of ν for one of the categories (ECAT). We would like to note that the path complexity was, 20,628, just barely more than the dimension (dictionary size). We plot on the left hand side of the figure in log-scale the support size as a function of ν . It seems that the support is monotonic in ν and there is a region where it grows linearly. However, a closer examination (right figure) reveals non-monotonic changes in the size of $|I_+ \cup I_-|$. Examining the individual sets we see that the overall tendency is to increase their size but “locally” an index may enter and exit the sets I_+ and I_- multiple times. This behavior further justifies the usage of the local tracking algorithm while ruling out approximate algorithms that enforce monotonicity of the sets I_+ and I_- .

7. Application to n-gram Models

In this section we demonstrate the potential of the maximum entropy relaxation path for building an n-gram model. We would like to note though that the goal of this section is to underscore the potential of the approach rather than to obtain state-of-the-art results on a concrete benchmark. We refer the reader to (Chen and Goodman, 1999) for an introduction to n-gram models. A context is a string $s = \omega_n \omega_{n-1} \dots \omega_1$ where each token w_i is from to an alphabet Ω . The tokens may be, for example, words in a dictionary, phonemes or, characters. In an n-gram model, the conditional probability $p(\cdot | \omega_n \dots \omega_1)$ over Ω is modelled using a variable-length Markov chain of fixed maximal length (Ron et al., 1996, Bühlmann and Wyner, 1999).

A convenient way to describe such models is by a suffix tree, whose nodes are tokens, such that paths from root to leaf determine a context Ω (see Figure 8(a)). Modern n-gram models are typically trained using a two-step procedure. First, a training buffer is used to count the number of occurrences of tokens in any given context: define $c(\omega | \omega_n \dots \omega_1)$ to be the number of occurrences of the string $\omega_n \dots \omega_1 \omega$ in the training buffer. These counts can be normalized to empirical distributions $q(\omega | \omega_n \dots \omega_1)$ over Ω and described by a function on the suffix tree (see again Figure 8(a)). These empirical distributions are just the maximum likelihood estimators for the underlying distributions on Ω . A parameter estimation of an n-gram model faces a classical bias-variance trade-off: each empirical distribution in a certain context is more accurate but also has a higher estimation variance than the empirical distribution in its shorter, parent context. To mitigate the variance of the estimates with the increase of the context length a second step, known as a *smoothing* or *back-off* is used. The second step is a specific recipe to combining or interpolating empirical distributions from different levels along each path from root to leaf on the suffix tree. The smoothing procedure often concludes with a secondary subprocess, called pruning, in which contexts whose estimated distribution is suspected to be inaccurate are removed from the final estimated model (Figure 8(b)).

N-gram models for machine translation and speech recognition, where the alphabet Ω is a significant subset of a natural language dictionary, can get quite large in

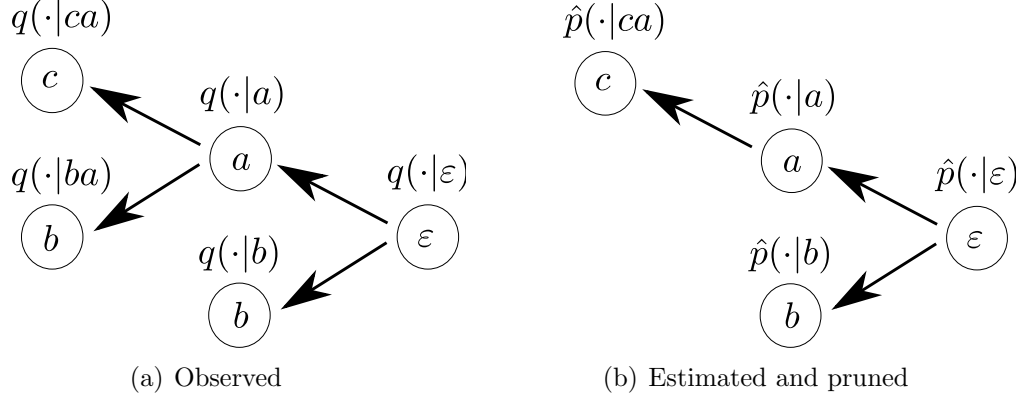


Figure 8: Estimation of an n-gram model represented by a suffix tree

terms of number of parameters (Brants et al., 2007). In trying to reduce the storage and retrieval burden imposed by prediction using a very large n-gram model, several compressed representations of n-gram models in general, and for those represented using suffix trees in particular, have been proposed, see for instance (Pauls and Klein, 2011). Alternatively, instead of asking to reduce the number of parameters by compacting an estimated model, one might wish to leave out parameters, whose inclusion in the model does not give sufficient improvement in performance. This idea leads to a procedure known as entropy-based pruning (Stolcke, 2000). In this section we propose a new approach in which the estimation and pruning procedures are two facets of the same process. Instead of pruning a fully estimated n-gram model, ideally we start with a given *parameter budget* and allocate parameters from the budget in the most advantageous way, as measured by likelihood of the model on a validation buffer. As we now show, the regularized maximum entropy problem offers a natural approach to the parameter allocation in an n-gram model.

Cascading relaxed maximum entropy problems. A first step towards an n-gram model based on relaxed maximum entropy problems is cascading a sequence of maximum entropy problems, where each problem receives as its “prior” distribution the solution of the problem that precedes it. Assume that we have a sequence of “empirical” distributions $\mathbf{q}^{(1)} \dots \mathbf{q}^{(s)}$ and a “prior” distribution \mathbf{u} on Ω . We cascade maximum entropy problems by taking, for the $i + 1$ -th problem, a specific solution $\mathbf{p}^{(i)}$ to the i -th problem as “prior” distribution and $\mathbf{q}^{(i+1)}$ as “empirical” distribution. Formally, for $i \geq 1$ let

$$\mathbf{p}^{(i)} = \operatorname{argmin}_{\mathbf{p} \in \Delta} \sum_{j=1}^n p_j \log \left(\frac{p_j}{p_j^{(i-1)}} \right) \quad \text{s.t.} \quad \|\mathbf{p} - \mathbf{q}^{(i)}\|_{\infty} \leq 1/\nu^{(i)},$$

where $\nu^{(i)}$ is our choice of relaxation parameter for the i -th problem. It is convenient to write $\mathbf{p}^{(0)} = \mathbf{u}$ and $Z^{(0)} = 1$. Denoting by $\boldsymbol{\alpha}^{(i)}$ the dual solution to $\mathbf{p}^{(i)}$, we have

$$p_j^{(i)} = \frac{p_j^{(i-1)} e^{\alpha_j^{(i)}}}{Z^{(i)}} \text{ where } Z^{(i)} = \sum_j p_j^{(i-1)} \exp(\alpha_j^{(i)}) .$$

The i -th solution thus has the form

$$p_j^{(i)} = \frac{\exp\left(\sum_{k=0}^i \alpha_j^{(k)}\right)}{\prod_{k=0}^i Z^{(k)}} .$$

Consequently, to store the distributions $\mathbf{p}^{(1)}, \dots, \mathbf{p}^{(s)}$, we need only store the dual solutions $\boldsymbol{\alpha}^{(1)}, \dots, \boldsymbol{\alpha}^{(s)}$, which tend to be sparse, and the normalization factors $Z^{(1)}, \dots, Z^{(s)}$.

Using the relaxation path for parameter allocation. We now describe a framework for parameter allocation and pruning in n -gram models. We use cascading of relaxed maximum entropy problems along paths from the root to leaf of a suffix tree, combined with the model selection procedure of Sec. 5. To set the notation, let us write $\mathbf{p}(\cdot|\omega_n \dots \omega_1)$ for the estimated probability distribution in the context $\omega_n \dots \omega_1$. This is a vector indexed by the token $\omega \in \Omega$, and we write $p(\omega|\omega_n \dots \omega_1)$ for the value it takes at ω . Similarly, let $\mathbf{q}(\cdot|\omega_n \dots \omega_1)$ denote the empirical distribution vector as calculated over the training buffer, let $\mathbf{r}(\cdot|\omega_n \dots \omega_1)$ be the empirical distribution vector in this context as calculated over a validation buffer, and let $\mathbf{p}(\cdot|\varepsilon)$ denote a given “prior” where ε denotes the empty context.

Suppose that we have determined the probability distribution $\mathbf{p}(\cdot|\omega_n \dots \omega_1)$, which our model uses for prediction in the context $\omega_n \dots \omega_1$. The task is to determine the distributions $\mathbf{p}(\cdot|\omega_{n+1} \dots \omega_1)$ in each of the sub-contexts of length $n + 1$. For each sub-context $\omega_{n+1} \dots \omega_1$, we solve for the entire relaxation path of the relaxed maximum entropy with “prior” distribution $\mathbf{p}(\cdot|\omega_n \dots \omega_1)$ and “observed” distribution $\mathbf{q}(\cdot|\omega_{n+1} \dots \omega_1)$. With the relaxation path available, we perform the efficient cross validation procedure of Sec. 5 against the validation distribution $\mathbf{r}(\cdot|\omega_{n+1} \dots \omega_1)$, and obtain a list of options in the form of Table 1. For the sub-context $\omega_{n+1} \dots \omega_1$, write $(k^{\omega_{n+1}}, L(k^{\omega_{n+1}}))$ for the option with model size $k^{\omega_{n+1}}$ and corresponding validation loss $L(k^{\omega_{n+1}})$. (The context $\omega_n \dots \omega_1$ is held fixed and implicit in this notation.) For each sub-context, each option in the list corresponds to a specific choice of prediction distribution in this context. To choose one option out of each list, an allocation rule is applied as discussed below. Let $\kappa^{\omega_{n+1}}$ denote the option chosen by the allocation rule for sub-context $\omega_{n+1} \dots \omega_1$. This results in a specific prediction distribution $\mathbf{p}(\cdot|\omega_{n+1} \dots \omega_1)$ for each sub-context, and decreases the total parameter budget by $\sum_{\omega_{n+1} \in \Omega} \kappa^{\omega_{n+1}}$. The remaining parameter budget is divided among the sub-contexts according to the allocation rule, and the algorithm proceeds recursively on each sub-context that received an allocation $\kappa^{\omega_{n+1}} > 0$, each with its own budget. The end

result is a compact exponential representation of a recursive form,

$$\begin{aligned} p(\omega|\omega_{n+1}\dots\omega_1) &\stackrel{\text{def}}{=} \frac{p(\omega|\omega_n\dots\omega_1)\exp(\alpha(\omega|\omega_{n+1}\dots\omega_1))}{Z(\omega|\omega_{n+1}\dots\omega_1)} \\ &= p(\omega|\varepsilon)\frac{\exp(\sum_{i=1}^{n+1}\alpha(\omega|\omega_i\dots\omega_1))}{\prod_{i=1}^{n+1}Z(\omega|\omega_i\dots\omega_1)}, \end{aligned}$$

where $Z(\omega|\omega_{n+1}\dots\omega_1)$ is the required normalizing factor and $\alpha(\omega|\omega_{n+1}\dots\omega_1)$ is the dual solution to $p(\omega|\omega_{n+1}\dots\omega_1)$. The sparsity of $\alpha(\cdot|\omega_{n+1}\dots\omega_1)$, namely the amount of parameters allocated to specializing $p(\cdot|\omega_n\dots\omega_1)$ to $p(\cdot|\omega_{n+1}\dots\omega_1)$ is chosen to give the best improvement in validation loss per parameter. We can thus estimate and store $p(\cdot|\omega_{n+1}\dots\omega_1)$ not as a distribution in its own right, but as an exponential tilt of the previously estimated distribution in the shorter context.

Parameter Allocation and Pruning. Unlike most well-known backoff or smoothing methods for training n-gram models, the approach proposed here does not contain a separate pruning procedure (Kneser, 1996) that is executed after the model has been trained in full. Instead, pruning happens naturally as part of parameter allocation. If the allocation rule set $\kappa^{\omega_{n+1}} = 0$ for the sub-context $\omega_{n+1}\dots\omega_1$, then this sub-context (as well as the sub-suffix-tree rooted at it) were pruned. The allocation κ^ω to a certain sub-context $\omega\omega_1\dots\omega_n$ may be understood as follows: according to the validation set, the benefit that can be expected from letting the distribution $p(\cdot|\omega_{n+1}\dots\omega_1)$ differ from $p(\cdot|\omega_n\dots\omega_1)$ is not worth allocating even a *single* parameter. We use a simple allocation rule in our experiments. We fixed a maximal tree depth N and a per-node budget b . We determined the allocation of each sub-context independently of the other sub-contexts. For sub-context $\omega_{n+1}\dots\omega_1$, if $N = n$, allocate $\kappa^{\omega_{n+1}} = 0$. Otherwise, choose the option $k^{\omega_{n+1}}$ with most parameters such that $k^{\omega_{n+1}} \leq b$. Namely, we allocated at most b parameters at each node (single maximum entropy problem). This allocation is rather rudimentary and its goal is mostly to demonstrate the potential of the maximum entropy relaxation path.

Evaluation. We have implemented our approach in a prototype character-based n-gram model. Such models, in which the alphabet Ω consists of a subset of the Unicode symbols, are commonly used in optical character recognition (OCR) applications in conjunction with an image processing module. The predicted probability provided by the n-gram model is combined with an image content score in order to determine the identity of the characters composing the image. Depending on the language, the alphabet size is on the order of thousands. The available data was a buffer of $40 \cdot 10^6$ characters from several languages. The last 20% of each buffer were held out and used as the validation set. Each n-gram model was trained according to the maximum entropy framework with the trivial allocation above. Different model sizes were achieved by tuning the maximal tree depth and the maximum parameter allocated to any individual maximum entropy problem. Performance of each model

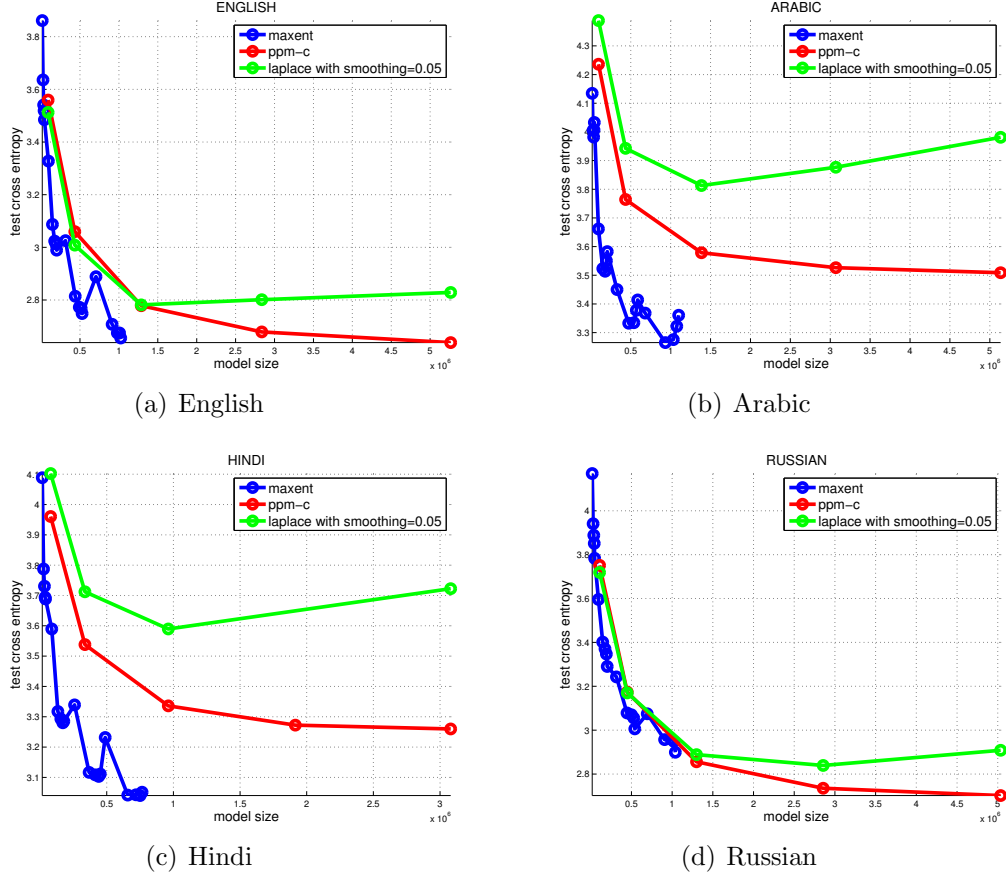


Figure 9: Character-based n-gram models: Comparison of cross-entropy performance on unseen test buffer

was measured using cross entropy against a new test buffer with approximately $1 \cdot 10^6$ characters. As a baseline, performance was compared against a Laplace (or “add-one”) smoothing model with a smoothing parameter held fixed at 0.05. Performance was compared against PPM-C (Moffat, 1990), one of the current method of choice for training character-based n-gram models. We capped the maximal depth of the trees obtained by Laplace smoothing and PPM-C in order to control their model size. The results are summarized in Figure 7. The plots show the trade-off of model size versus performance. We do not expect that the method proposed here would outperform state of the art when the model size is unlimited. Rather, we expect it to provide a favorable size versus performance trade-off, particularly in the regime where model size is severely restricted. Our results seem to support this hypothesis. Indeed, we see that especially for Hindi and Arabic we can achieve low out of sample entropy for very small model sizes.

8. Extensions

In the previous sections we focused on tracking algorithms for the important case where the separable objective function is the relative entropy. In this section we discuss a simple but useful extension of the problem that builds on the multiplicity vector \mathbf{m} . In addition, we describe an adaptation of our tracking algorithm for another setting where the master equation $G(\nu, \mu) = 0$ can be solved efficiently, namely the squared Euclidean distance.

Coordinate-weighted relaxation. The observed distribution, as its name implies, is often a rational distribution obtained through dividing the number of observations of each event from the multinomial distribution by the total number of observations. It is therefore desirable to impose different constraints on the differences $|p_j - q_j|$ so as to accommodate the number of observations. For instance, when $q_j = 0$, we simply have not observed any events corresponding to the j -th outcome. In this case, it is typically desirable to enforce a stricter difference on $|p_j - q_j|$. Formally, we would like to associate an a priori accuracy parameter δ_j such that

$$\forall j \in [n] : |p_j - q_j| \leq \frac{\delta_j}{\nu} , \quad (31)$$

and perform tracking of all admissible values of ν as before. As we now show, we can use the multiplicity vector in place of $\boldsymbol{\delta}$ to handle this setting as long as \mathbf{q} and \mathbf{u} are in the simplex (without multiplicity). Note while we motivated \mathbf{m} as a multiplicity vector, the sole requirement we placed on \mathbf{m} is positivity, namely, $m_j > 0$ for all $j \in [n]$. We next set $\mathbf{m} = \boldsymbol{\delta}$ and define $\tilde{p}_j = p_j/m_j$, $\tilde{q}_j = q_j/m_j$, $\tilde{u}_j = u_j/m_j$. The resulting problem becomes,

$$\min_{\tilde{\mathbf{p}} \in \Delta(\mathbf{m})} \sum_{j=1}^n m_j \tilde{p}_j \log \left(\frac{\tilde{p}_j}{\tilde{u}_j} \right) \quad \text{s.t.} \quad \|\tilde{\mathbf{p}} - \tilde{\mathbf{q}}\|_\infty \leq 1/\nu ,$$

where $\tilde{\mathbf{q}}, \tilde{\mathbf{u}} \in \Delta(\mathbf{m})$. Clearly, the above problem is of exactly the same form of (13). To recap, by setting the multiplicity \mathbf{m} to be the a-priori relaxation vector $\boldsymbol{\delta}$ we can straightforwardly accommodate constraints of the form (31) while performing relaxation path tracking.

Relaxation Path for Square Loss. We next focus on examining a different choice for $\phi(\cdot)$ and review the required changes to the core of the tracking procedure. The objective function we examine is the squared Euclidean distance between \mathbf{p} and \mathbf{u} . The optimization problem is

$$\min_{\mathbf{p} \in \Delta(\mathbf{m})} \frac{1}{2} \sum_{j=1}^n (p_j - u_j)^2 \quad \text{s.t.} \quad \|\mathbf{p} - \mathbf{q}\|_\infty \leq 1/\nu \quad (32)$$

where $\mathbf{q}, \mathbf{u} \in \Delta(\mathbf{m})$. This problem is concerned with projecting \mathbf{u} into the intersection of the ℓ_1 and ℓ_∞ polytopes. Note that by modifying \mathbf{m} we can control the size of

the ℓ_1 ball in which \mathbf{p} should reside. In the interest of simplicity we now assume $\mathbf{m} \equiv 1$. The objective function in this problem is clearly of the form given by (8) with $\phi_j(p_j) = \frac{1}{2}(p_j - u_j)^2$. Recalling the construction from Sec. 2.3, we need to calculate $d\phi_j(p_j)/dp_j$ and find its inverse. Since

$$\frac{d\phi_j(p_j)}{dp_j} = p_j - u_j$$

the inverse function ψ_j must satisfy

$$\psi_j(p_j - u_j) = p_j \quad .$$

Denoting $\eta = p_j - u_j$ we get that $\psi_j(\eta) = u_j + \eta$. Next, we can expand (10) and write

$$p_j = q_j + \frac{1}{\nu} \theta(\nu(u_j + \eta) - \nu q_j) \quad .$$

We define $\mu = \nu\eta$ and get that the dependency of \mathbf{p} is piece-wise linear in (ν, μ) as follows,

$$p_j = q_j + \frac{1}{\nu} \theta(\nu(u_j - q_j) + \mu) \quad .$$

We now define \mathcal{M} as before and introduce the following definitions,

$$\mathcal{R} = \sum_{j \in I_0} u_j - q_j \quad , \quad \mathcal{B} = |I_0| \quad .$$

Then, the requirement that $G(\nu, \mu) = 0$ yields = ANSWER: FIXED the following linear equation,

$$\nu\mathcal{R} + \mu\mathcal{B} + \mathcal{M} = 0 \quad ,$$

which forms the equation for the line ℓ_0 . We can now repeat the tracking procedure almost verbatim and perform projections onto the intersection of the ℓ_1 ball with the hypercube of length $1/\nu$ centered at \mathbf{q} for all possible values of ν . This solution is an entire relaxation path generalization of the projection procedure onto the $\ell_{1,\infty}$ polytopes as described in (Quattoni et al., 2009).

Acknowledgments

We thank John Duchi, Sally Goldman, Han Liu, and Fernando Pereira for valuable feedback. Thanks to John Blitzer for comments and suggestions on the final manuscript. MG was partially supported by a William R. and Sara Hart Kimball Stanford Graduate Fellowship and conducted this work while at Google Research.

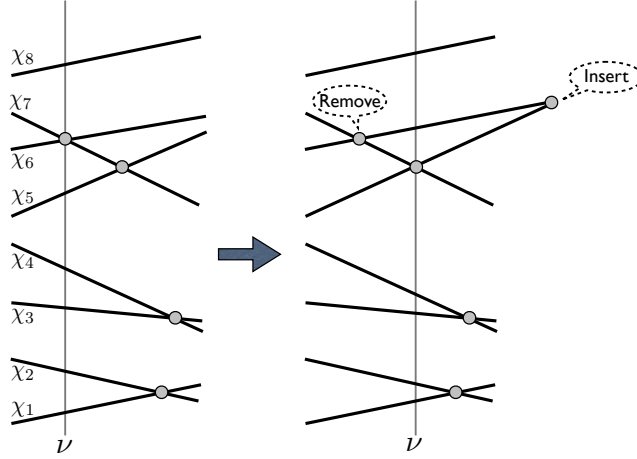


Figure 10: Illustration of the line scanning process during a single iteration of the global homotopy tracking.

Appendix A. Global Homotopy Tracking

The local homotopy tracking algorithm repeatedly calculates the intersection of ℓ_0 with *all* of the lines $\ell_{\pm j}$, regardless of their orientation. Thus, computing the intersections of ℓ_0 with the lines $\ell_{\pm j}$ requires $O(n)$ operations. In this section we present an alternative algorithm that maintains a global view of all of the lines including the line ℓ_0 . The global homotopy tracking requires though a more complex data structure, namely a priority queue (Cormen et al., 2001), that facilitates insertions and deletions in $O(\log(n))$ time and finding the smallest element in the data structure in constant time.

The global algorithm scans the (ν, μ) plane left to right, starting with $\nu = 0$, while maintaining the intersections of the lines $\ell_{\pm j}$ and ℓ_0 with a vertical line placed at ν . We denote by ℓ_ν the vertical line located at ν . Throughout the scanning process we maintain a priority queue for reasons that are explained shortly. We denote by χ the vector which records the order in which the lines $\ell_{\pm j}$ and ℓ_0 intersect the horizontal line ℓ_ν (see also Fig. 10). Formally, the vector χ records for a given ν the vertical intersections such that $\mu_{\chi_0} \leq \mu_{\chi_2} \leq \dots \leq \mu_{\chi_{2n}}$ where

$$(\nu, \mu_j) = \ell_j \cap \ell_\nu \quad \text{for } -n \leq j \leq n \quad .$$

Note that the line ℓ_0 which defines the solution is treated as any other line ℓ_j for $1 \leq |j| \leq n$. Naturally, our procedure would take a few additional steps when the scanning process is concerned with ℓ_0 , as we describe in the sequel.

The definition of χ implies that adjacent lines on ℓ_ν intersect at

$$(\tilde{\nu}_i, \tilde{\mu}_i) = \ell_{\chi_{i-1}} \cap \ell_{\chi_i} \quad ,$$

where $1 \leq i \leq 2n$. We use a priority queue to keep track of future intersections. The intersections where $\tilde{\nu}_i \leq \nu$ have already been observed and no longer reside in the priority queue. The pairs $(\tilde{\nu}_i, i)$ where $\tilde{\nu}_i > \nu$ are arranged in the priority queue in an increasing order, so that the smallest $\tilde{\nu}_i > \nu$ is at the front of the priority queue. For each element $\tilde{\nu}_i$ we also keep the index i in order to retrieve the line the intersection corresponds to in a constant time. During the scanning process we also maintain the variables $\mathcal{M}, \mathcal{U}, \mathcal{Q}$ which describe the current segment of ℓ_0 . We start at $\nu = 0$, $\mathcal{M} = 0$, $\mathcal{U} = \mathcal{Q} = 1$ and populate the priority queue. The tracking process involves the following iterates. We pull out the minimal pair $(\tilde{\nu}_i, i)$ from the priority queue. The value $\tilde{\nu}_i$ corresponds to the intersection of the line $\ell_{\chi_{i-1}}$ and ℓ_{χ_i} .

Let us examine first the case where both $\chi_i \neq 0$ and $\chi_{i-1} \neq 0$. In this case the two lines simply switch their position on the scan line ℓ_ν as ν passes through $\tilde{\nu}_i$. We thus need to swap χ_i and χ_{i-1} in χ . Moreover, the intersection $\tilde{\nu}_{i-1}$ and $\tilde{\nu}_{i+1}$ become outdated due to the swap in positions. We locate their indices using the back-pointers on the priority queue and take them out of the priority queue. (Note that neither of them must reside in the queue since we might have encountered these values earlier during the scanning process.) Since the lines changed their order, there might be newly formed intersections looming ahead. These intersections, $\tilde{\nu}_{i-1}$ and $\tilde{\nu}_{i+1}$, are computed and added to the queue if they are larger than $\tilde{\nu}_i$. In Fig. 6 we illustrate the process of updating the priority queue when processing the current element at the top of the queue.

When either $\chi_i = 0$ or $\chi_{i-1} = 0$ extra measures need to be taken since we encounter an intersection of the line ℓ_0 with one of the lines $\ell_{\pm j}$ for $j \geq 1$. First, we add a new line segment to $\mu(\nu)$ originating at $(\tilde{\nu}_i, \tilde{\mu}_i)$. We next update $\mathcal{M}, \mathcal{U}, \mathcal{Q}$ as required by the intersection in the same way the update is performed when conducting the local homotopy tracking. Now that we have the updated slope of ℓ_0 available, we can proceed and calculate potential new intersections with the neighboring (above and below) lines and add them to the priority queue in case their value is larger than $\tilde{\nu}_i$.

The global homotopy tracking finishes when the queue is empty. It requires $O(n)$ storage and $O(n^2 \log(n))$ operations since each insertion and deletion from the queue can be performed in $O(\log(n))$ steps. Clearly, if the number of line segments constituting $\mu(\nu)$ is greater than $n \log(n)$ (recall that the upper bound is $O(n^2)$) then the global homotopy procedure is faster than the local one.

Example Since the global tracking process is somewhat complex, we now give a concrete example which illustrates the process. We examine the following toy problem setting,

$$\mathbf{u} = \left(\frac{1}{2}, \frac{1}{8}, \frac{1}{12} \right) \quad , \quad \mathbf{q} = \left(\frac{1}{4}, \frac{1}{3}, \frac{1}{36} \right) \quad , \quad \mathbf{m} = (1, 2, 3) \quad .$$

At the start we set $\nu = 0$, $\mathcal{M} = 0$, $\mathcal{U} = \mathcal{Q} = 1$, and $\chi = (-3, -2, -1, 0, 1, 2, 3)$. The queue contains the following pairs of values and back-indices,

$$(12/7, 6) \quad , \quad (36/13, 2) \quad , \quad (4, 4) \quad .$$

Next we pull $(12/7, 6)$ from the front of the queue and set $\nu \leftarrow 12/7$. We reorder χ and set $\chi \leftarrow (-3, -2, -1, 0, 1, 3, 2)$. Last for this intersection point, we remove $(12/7, 6)$ and add a newly found intersection, so that the priority queue becomes,

$$(36/13, 2) \quad , \quad (4, 4) \quad , \quad (60, 5) \quad .$$

We next pull $(36/13, 2)$ out of the queue, thus setting $\nu \leftarrow 36/13$. The last removal results in the following line ordering $\chi \leftarrow (-3, -1, -2, 0, 1, 3, 2)$. We also identify a new line intersection and the queue becomes,

$$(4, 4) \quad , \quad (24/5, 3) \quad , \quad (60, 5) \quad .$$

We then remove $(4, 4)$ from the front of the queue, setting $\nu \leftarrow 4$, the line ordering $\chi \leftarrow (-3, -1, -2, 1, 0, 3, 2)$, and the queue to contain the following pairs

$$(60/13, 3) \quad , \quad (15, 5) \quad .$$

One of the lines at the current intersection ($\nu = 4$) is ℓ_0 we thus perform the update

$$\mathcal{M} \leftarrow 1 \quad , \quad \mathcal{U} \leftarrow \frac{1}{2} \quad , \quad \mathcal{Q} \leftarrow \frac{3}{4} \quad .$$

The global homotopy tracking continues the above schemes and goes through numerous more line intersections.

References

- J. Blitzer, M. Dredze, and F. Pereira. Biographies, Bollywood, boom-boxes and blenders: domain adaptation for sentiment classification. In *Association for Computational Linguistics*, 2007.
- Thorsten Brants, Ashok C. Popat, Peng Xu, Franz J. Och, Jeffrey Dean, and Google Inc. Large language models in machine translation. In *In EMNLP*, pages 858–867, 2007.
- P. Bühlmann and A.J. Wyner. Variable length markov chains. *The Annals of Statistics*, 27(2):480–513, 1999.
- E.J. Candés and T. Tao. Near optimal signal recovery from random projections: Universal encoding strategies? *IEEE Transactions on Information Theory*, 52(12):5406–5425, 2006.
- S.F. Chen and J. Goodman. An empirical study of smoothing techniques for language modeling. *Computer Speech & Language*, 13(4):359–393, 1999.
- Thomas H. Cormen, Charles E. Leiserson, Ronald L. Rivest, and Clifford Stein. *Introduction to Algorithms*. MIT Press, 2001.

- D.L. Donoho. Compressed sensing. *IEEE Transactions on Information Theory*, 52(4):1289–1306, 2006.
- M. Dudík, S. J. Phillips, and R. E. Schapire. Maximum entropy density estimation with generalized regularization and an application to species distribution modeling. *Journal of Machine Learning Research*, 8:1217–1260, June 2007.
- Bradley Efron, Trevor Hastie, Iain Johnstone, and Robert Tibshirani. Least angle regression. *Annals of Statistics*, 32(2):407–499, 2004.
- T. Hastie, S. Rosset, R. Tibshirani, and J. Zhu. The entire regularization path for support vector machine. *Journal of Machine Learning Research*, 5:1391–1415, 2004.
- R. Kneser. Statistical language modeling using a variable context length. In *Spoken Language, 1996. ICSLP 96. Proceedings., Fourth International Conference on*, volume 1, pages 494–497. IEEE, 1996.
- A. Moffat. Implementing the ppm data compression scheme. *Communications, IEEE Transactions on*, 38(11):1917–1921, 1990.
- Michael R. Osborne, Brett Presnell, and Berwin A. Turlach. On the lasso and its dual. *Journal of Computational and Graphical Statistics*, 9(2):319–337, 2000a.
- M.R. Osborne, B. Presnell, and B.A. Turlach. A new approach to variable selection in least squares problems. *IMA journal of numerical analysis*, 20(3):389–403, 2000b.
- M.Y. Park and T. Hastie. L1-regularization path algorithm for generalized linear models. *Journal of the Royal Statistical Society: Series B (Statistical Methodology)*, 69(4):659–677, 2007.
- A. Pauls and D. Klein. Faster and smaller n-gram language models. In *Proceedings of the 49th Annual Meeting of the Association for Computational Linguistics: Human Language Technologies-Volume 1*, pages 258–267. Association for Computational Linguistics, 2011.
- M. Pontil and A. Verri. Properties of support vector machines. *Neural Computation*, 10(4), 1998.
- A. Quattoni, X. Carreras, M. Collins, and T. Darrell. An efficient projection for L1, infinity regularization. In *Proceedings of the 26th International Conference on Machine Learning*, 2009.
- L. Rabiner and B.H. Juang. *Fundamentals of Speech Recognition*. Prentice Hall, 1993.
- Dana Ron, Yoram Singer, and Naftali Tishby. The power of amnesia: learning probabilistic automata with variable memory length. *Machine Learning*, 25(2):117–150, 1996.

- S. Rosset. Tracking curved regularized optimization solution paths. In *Advances in Neural Information Processing Systems 17*, 2004.
- S. Rosset and J. Zhu. Piecewise linear regularized solution paths. *The Annals of Statistics*, 35(3):1012–1030, 2007.
- A. Stolcke. Entropy-based pruning of backoff language models. *Arxiv preprint cs/0006025*, 2000.
- R. Tibshirani. Regression shrinkage and selection via the lasso. *Journal of the Royal Statistical Society: Series B*, 58(1):267–288, 1996.
- R.J. Tibshirani and J. Taylor. The solution path of the generalized lasso. *The Annals of Statistics*, 39(3):1335–1371, 2011.
- P. Zhao and B. Yu. Boosted lasso. Technical report, University of California, Berkeley, 2004.